Journal of Molecular Medicine
https://doi.org/10.1007/s00109-021-02103-0

ORIGINAL ARTICLE

Zinc finger and BTB domain-containing protein 20 aggravates angiotensin II-induced cardiac remodeling via the EGFR-AKT pathway

Fangfang Li[1,2] · Miaomiao Du[1,2] · Yiming Yang[1,2] · Zhu Wang[1,2] · Hu Zhang[1,2] · Xiaoyu Wang[1,2] · Qing Li[1,2]

Received: 28 January 2021 / Revised: 5 June 2021 / Accepted: 10 June 2021

Abstract

Zinc finger and BTB domain-containing protein 20 (ZBTB20) play an important role in glucose and lipid homeostasis. ZBTB20 was shown to be a crucial protein for the maintenance of cardiac contractile function. However, the role of ZBTB20 in cardiac response remodeling has not been elucidated. Thus, this study aimed to explore the role of ZBTB20 in cardiac remodeling following angiotensin II insult. Mice were subjected to angiotensin II infusion to induce a cardiac adverse remodeling model. An adeno-associated virus (AAV) 9 system was used to deliver ZBTB20 to the mouse heart. Here, we demonstrate that ZBTB20 expression is elevated in angiotensin II-induced cardiac remodeling and in response to cardiomyocyte insults. Furthermore, AAV9-mediated overexpression of ZBTB20 caused cardiac wall hypertrophy, chamber dilation, increased fibrosis, and reduced ejection fraction. Additionally, ZBTB20 siRNA protected cardiomyocytes from angiotensin II-induced hypertrophy. Mechanistically, ZBTB20 interferes with EGFR and Akt signaling and modulates the remodeling response. Overexpression of constitutively active Akt counteracts ZBTB20 knockdown-mediated protection of adverse cardiac remodeling. These findings illustrate the role of ZBTB20 in the transition of adverse cardiac remodeling toward heart failure and provide evidence for the molecular programs inducing adverse cardiac remodeling.

Key messages

- ZBTB20 is a transcription factor from the POK family.
- ZBTB20 is upregulated in heart tissue treated with angiotensin II.
- ZBTB20 influences cardiomyocyte hypertrophy via the EGFR-Akt pathway.
- Akt continuous activation leads to similar results to ZBTB20 overexpression.

Keywords ZBTB20 · Adverse cardiac remodeling · Angiotensin II · EGFR · Akt

Introduction

Cardiac remodeling plays a vital role in the cardiovascular disease process of heart failure. Initially, remodeling alterations help compensate for cardiac performance; however, over time, these compensatory mechanisms often lead to pump failure [1]. Pressure overload, myocarditis, myocardial ischemia and infarction, and hypertension can lead to adverse remodeling. Neurohumoral activation is the most common mechanism for initiating and accelerating adverse remodeling progress in these diseases [2]. Excessive circulating and tissue angiotensin II (AngII) as well as increased aldosterone levels lead to a profibrotic, proinflammatory, and prohypertrophic milieu that causes remodeling and dysfunction of cardiovascular tissues [2]. Thus, the administration of angiotensin-converting enzyme inhibitors (ACEIs) and AngII type 1 receptor blockers (ARBs) represents one of the main strategies in heart failure treatment [3]. However, the mechanism that bypasses these therapeutic blockades and reduces their efficacy is poorly understood [2]. Thus, it is necessary to improve our understanding of this system and more adeptly modulate it to improve clinical outcomes.

AngII binds to AngII type 1 receptor (AT1R), leading to both prohypertrophic and profibrotic effects by transactivating EGFR in the heart [4]. Following AngII-induced activation, AT1R was shown to mediate EGFR phosphorylation and to activate ERK and Akt. Studies have shown that EGFR inhibition can impair diverse factors capable of inducing adverse cardiac remodeling [5–7]. AngII-induced

✉ Qing Li
liqing6565@126.com

[1] Department of Cardiothoracic Surgery, The Affiliated Hospital of Xuzhou Medical University, Xuzhou, Jiangsu Province 221000, People's Republic of China

[2] Jiangsu Provincial Institute of Health Emergency, Xuzhou Medical University, Xuzhou 221000, China

Published online: 07 July 2021

cardiac fibroblast activation is also mediated by EGFR activation [8]. Thus, targeting AngII-induced EGFR signaling may represent a promising method to treat both cardiac hypertrophy and fibrosis during the adverse remodeling process.

Zinc finger and BTB domain-containing protein 20 (ZBTB20) is a member of the POK family, which contains a conserved C_2H_2 Krüppel-type zinc finger and BTB/POZ domains [9]. It regulates many physiological functions by acting as a transcriptional repressor for lipid and glucose homeostasis [10], neurodevelopment [9], immune response [11], and cancer development [12]. Recently, Zhang et al. [13] reported that ZBTB20 was involved in hepatocyte proliferation, which indicated its involvement in survival and proliferation. Ren et al. [14] reported that ZBTB20 deficiency leads to a reduction in heart size and hypotension. This suggests that ZBTB20 plays a role in maintaining normal function and may participate in the progression of cardiovascular disease. AngII, as one of the most proremodeling neurohumoral factors, was proven to induce cardiac hypertrophy, cardiac fibrosis, and inflammation as well as vascular dysfunction. Thus, in this study, we used AngII infusion to establish a cardiac remodeling model [15–17]. In this study, we aimed to elucidate the functional role of ZBTB20 in adverse cardiac remodeling induced by AngII.

Methods

Animals

The Institute of Laboratory Animal Science, Chinese Academy of Medical Sciences (Beijing, China), supplied adult male C57BL/6 mice (8–10 weeks old). The Guide for the Care and Use of Laboratory Animals published by the US National Institutes of Health was applied to all animal procedures in our experiment, and approval from the Institutional Animal Care and Use Committee at Xuzhou Medical University (Xuzhou, China) was also acquired. Mice were divided into four groups: AAV9-negative control (NC) + normal saline (NS) group (n = 15), AAV9-ZBTB20 + NS group (n = 15), AAV9-NC + AngII group (n = 15), and AAV9-ZBTB20 + AngII group (n = 15). Mice were subjected to AAV9-ZBTB20 or AAV9-NC injection 2 weeks before AngII infusion. To knock down ZBTB20, mice were injected with AAV9-shZBTB20 2 weeks before AngII infusion. To constitutively activate (ca.) Akt, mice were injected with adenovirus (Ad)-ca. Akt. In the mechanism-exploring experiment, mice were divided into three groups: AAV9-NC-AngII group (n = 15), AAV9-shZBTB20-AngII group (n = 15), and AAV9-shZBTB20 + AngII + Ad-ca. Akt group (n = 15).

Animal model

The mouse cardiac remodeling model was induced using 1.4 mg/kg AngII per day dissolved in 0.9% NaCl infused subcutaneously for 4 weeks using an osmotic minipump (Alzet model 2004, Alza Corp., Mountain View, CA, USA). Saline-infused animals served as infusion controls and were subjected to the same procedures as the experimental animals, except the AngII infusion.

Recombinant adeno-associated virus 9 construction

AAV9-ZBTB20, AAV9-shZBTB20, and AAV9-NC were constructed and generated by Vigene Biosciences (Shandong, China). The sequences of ZBTB20 shRNA oligos and negative controls (NC) are as follows: ZBTB20 (5′-CUAUGCGAUUACGACUAAGU-3′) and NC (5′-UUAGCAGUAUGGCAUACUAG-3′). The ZBTB20 mouse gene was cloned into the p-ENTER vector using the AsiS I and Mlu I restriction sites. The p-ENTER plasmid containing the desired gene and the AAV vector pAV-C-GFP were cotransfected into 293 cells to obtain the pAAV-MCS plasmid. Next, the recombinant plasmid pAAV-MCS was transfected into AAV-293 cells. Three days after transfection, AAV9 vector-producing 293 T cells were harvested for vector purification. Real-time PCR was performed to quantify the AAV viral particles. Adenovirus vectors carrying constitutively active AKT1 (Ad-ca. Akt) and GFP (Ad-GFP) were generated by Hanbio Biotechnology Co. (Shanghai, China).

Viral delivery protocol

Mice received a heart injection of AAV9-ZBTB20, AAV9-shZBTB20, AAV9-NC (1×10^{11} viral particles) or Ad-ca. Akt (1×10^{9} viral genome particles) 2 weeks before surgery. For surgery preparation, 3% pentobarbital sodium (80 mg/kg, intraperitoneal) was administered for anesthetization, and a rodent ventilator was used to maintain artificial respiration. The left pleural cavity was opened between the left third and fourth ribs and the pericardium. A 29-gauge syringe was used for injection through the apical, anterior, and lateral walls of the left ventricle (10 μl for each site). Following the procedure, the chest was closed, and mice were administered 0.5% bupivacaine for pain relief.

Echocardiographic and hemodynamic evaluation

Transthoracic echocardiography and hemodynamic analyses were used as previously described [18]. Isoflurane at 1.5% was

used to anesthetize the mice. Echocardiography was performed using a 10-MHz linear-array ultrasound transducer. A microtip catheter transducer was used for hemodynamic measurements. Signals were recorded using a Millar pressure–volume system.

Cardiac morphology and histomorphometric analysis

Cardiac morphology and histomorphometric analysis were performed as previously described [18]. Hematoxylin and eosin (H&E) staining was used to measure the cell surface area of more than 200 cells in each group. Picrosirius red (PSR) staining was performed to measure the LV collagen volume with more than 10 fields for each heart. The cross-sectional area (CSA) of the cells was analyzed using a quantitative digital imaging system based on Image-Pro Plus 6.0. Heart sections were also incubated with anti-CD68 (ABclonal, A6554) and anti-4-hydroxynonenal (4-HNE) (Abcam, ab-46545) for immunohistochemistry staining with a DAB detection kit.

Quantitative polymerase chain reaction

Total RNA was extracted from frozen mouse cardiac tissue or cardiomyocytes using TRIzol (15,596–026; Invitrogen, Carlsbad, CA, USA). RNA (2 μg from each sample) was reverse transcribed into cDNA using oligo (DT) primers and a Transcriptor First Strand cDNA Synthesis Kit (04,896,866,001; Roche). PCR amplifications in all groups were quantified using LightCycler 480 SYBR Green 1 Master Mix (04,707,516,001; Roche), and the results were normalized against glyceraldehyde-3-phosphate dehydrogenase (GAPDH) gene expression. The primers used are listed in Table 1.

Western blotting

Ice-cold radioimmunoprecipitation assay buffer (containing 50 mM Tris–HCl, 150 mM NaCl, 1% Triton X-100, 1% sodium deoxycholate, and 0.1% SDS) was used to extract proteins from cardiomyocytes and heart tissue. Next, the proteins were separated using 10% SDS-PAGE (50 μg per sample). After being transferred onto Immobilon membranes (Millipore, Billerica, MA, USA), proteins were incubated with primary antibodies overnight at 4 °C. The following primary antibodies were used: ZBTB20 (#ab243143, 1:1000 dilution) was purchased from Abcam (Cambridge, MA, USA); total (T)-Akt (#4691), phospho (P)-Akt (#4060), T-mTOR (Thr845) (#2983), P-mTOR (#2971), and GAPDH (#2118) were purchased from Cell Signaling Technology (Danvers, MA, USA) (1:1000 dilution); and P-EGFR (Tyr1173) (sc12351, diluted) and EGFR (sc31155, 1:200 diluted) were purchased from Santa Cruz Biotech (Santa Cruz, CA, USA). The blots were developed with enhanced chemiluminescence (ECL) reagents (Bio-Rad, Hercules, CA, USA) and captured using a ChemiDoc MP Imaging System (Bio-Rad). GAPDH was used as a loading control.

Cardiomyocyte culture

Neonatal rat cardiomyocytes (NRCMs) were cultured as described previously [18]. Briefly, 1- to 2-day-old Sprague–Dawley rats were sacrificed by cervical dislocation. Hearts were quickly removed, and the ventricles were washed with PBS three times and incubated with 0.125% trypsin–EDTA (Gibco, 2520–072, Grand Island, NY, USA) for 15 min. Ventricles were then enzymatically digested four times for 15 min in 0.125% trypsin–EDTA in PBS. Digestion was stopped by adding FBS at a final concentration of

Table 1 Primer sequences used for qPCR

mRNA	Forward	Reverse
ANP[a]	ACCTGCTAGACCACCTGGAG	CCTTGGCTGTTATCTTCGGTACCGG
BNP[a]	GAGGTCACTCCTATCCTCTGG	GCCATTTCCTCCGACTTTTCTC
β-MHC[a]	CCGAGTCCCAGGTCAACAA	CTTCACGGGCACCCTTGGA
Col1agenI[a]	AGGCTTCAGTGGTTTGGATG	CACCAACAGCACCATCGTTA
Col1agenIII[a]	AAGGCTGCAAGATGGATGCT	GTGCTTACGTGGGACAGTCA
α-SMA[a]	TTTCATTGGGATGGAGTCAGCG	GACAGGACGTTGTTAGCATAGAGA
TNF-α[a]	CATCTTCTCAAAATTCGAGTGACAA	TGGGAGTAGACAAGGTACAACCC
IL-1[a]	CCGTGGACCTTCCAGGATGA	GGGAACGTCACACACCAGCA
IL-6[a]	AGTTGCCTTCTTGGGACTGA	TCCACGATTTCCCAGAGAAC
GAPDH[a]	ACTCCACTCACGGCAAATTC	TCTCCATGGTGGTGAAGACA
ANP[a]	AAAGCAAACTGAGGGCTCTGCTCG	TTCGGTACCGGAAGCTGTTGCA
β-MHC[b]	TCTGGACAGCTCCCCATTCT	CAAGGCTAACCTGGAGAAGATG
GAPDH[b]	GACATGCCGCCTGGAGAAAC	AGCCCAGGATGCCCTTTAGT

Sequences are listed 5′–3′

[a]Mouse heart

[b]Rat cardiomyocytes

10%. Next, the cells were centrifuged at 250 × *g* for 8 min and resuspended in DMEM/F12 (Gibco, C11330) supplemented with 10% FBS. The resuspended cells were incubated for 1–2 h in a 100-mm dish to allow noncardiomyocytes (mainly cardiac fibroblasts) to adhere to the plastic. Next, the cells were seeded into six-well plates at a density of 5×10^5 cells per well with 1% bromodeoxyuridine for 48 h. Cells were transfected with Ad-ZBTB20 (MOI = 50) or ZBTB20 siRNA for 8 h to overexpress or knock down ZBTB20, respectively [19]. NRCMs were pretreated with 10 μM erlotinib (an EGFR inhibitor) for 30 min and then treated with AngII for 48 h. Cells were infected with Akt siRNA for 8 h to knockdown Akt.

Luciferase reporter assay

The luciferase reporter plasmids for the rat Egfr promoter (~3.7 kb) were cloned from rat genomic DNA using PCR and inserted into the pGL4.1 vector (Promega, Madison, WA, USA). Primary NRCMs were transfected with plasmids as well as Ad-ZBTB20 (Ad-NC as control) or ZBTB20 siRNA (ScRNA as control) using Lipofectamine 3000 (Invitrogen). After 48 h of transfection, cells were harvested and disrupted, and the luciferase activity was analyzed using the dual luciferase assay kit (Promega) and normalized against the activity of Renilla luciferase.

Statistical analysis

All data are expressed as the mean ± SD. Differences between groups were measured using two-way analysis of variance followed by Tukey's post hoc test. Comparisons between two groups were analyzed using an unpaired Student's *t*-test. *P*-values < 0.05 were considered statistically significant.

Results

Expression level of ZBTB20 in AngII-insulted hearts

To evaluate the association between ZBTB20 and cardiac remodeling, we established an AngII infusion-induced adverse cardiac remodeling mouse model. Furthermore, we detected the expression level of ZBTB20 in heart tissue. ZBTB20 protein levels were upregulated at 4 weeks following AngII infusion compared with those in control mouse hearts (Fig. 1a). Next, we isolated different cells from the hearts of mice that had undergone 4 weeks of AngII infusion to elucidate the role of ZBTB20. We found that in cardiomyocytes isolated from hearts treated with AngII for 4 weeks, the ZBTB20 protein level increased markedly (Fig. 1b). However, the expression of ZBTB20 did not change in fibroblasts or endothelial cells isolated from hearts treated with AngII for 4 weeks (Fig. 1c, d).

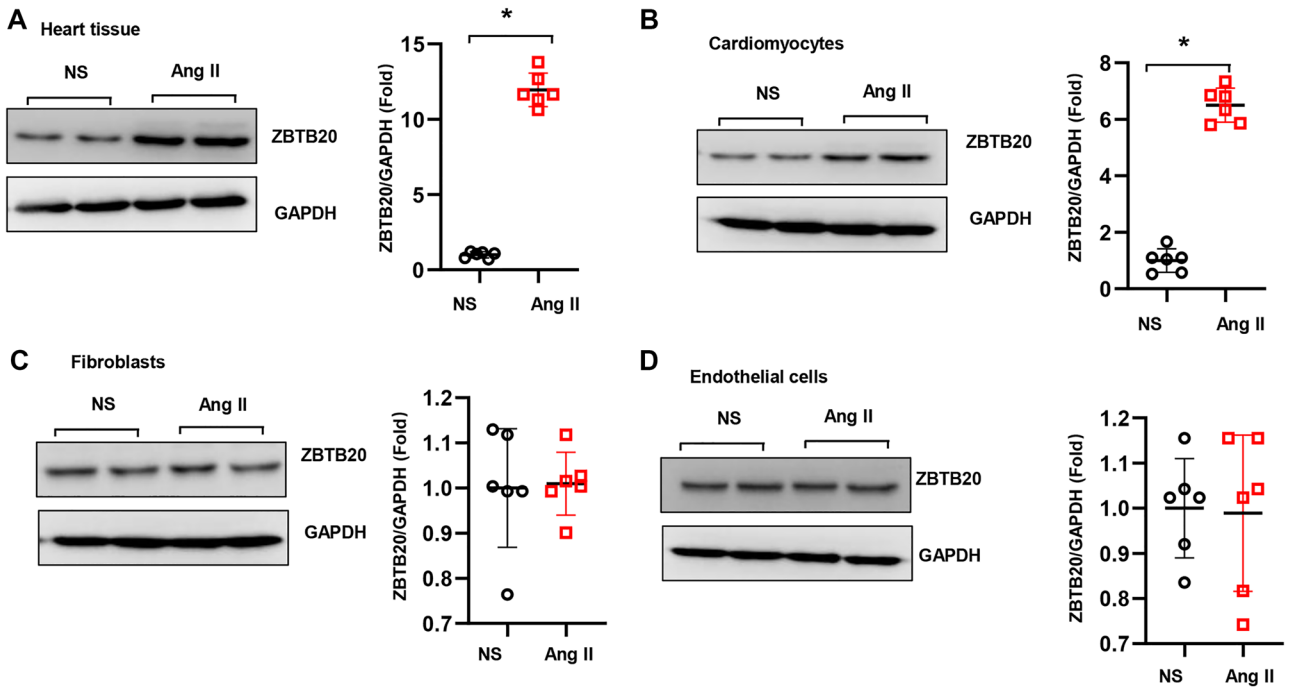

Fig. 1 Expression level of ZBTB20 in AngII-insulted hearts. **a** Mouse heart ZBTB20 protein levels in each group (n = 6). **b** ZBTB20 protein levels in cardiomyocytes isolated from mouse hearts 4 weeks after AngII infusion (n = 6). **c** ZBTB20 protein levels in fibroblasts isolated from mouse hearts 4 weeks after AngII infusion (n = 6). **d** ZBTB20 protein levels in endothelial cells isolated from mouse hearts 4 weeks after AngII infusion (n = 6). NS normal saline. **P* < 0.05. Unpaired Student's *t*-tests were used in Fig. 1a–d

These data suggest that ZBTB20 may play a role in adverse cardiac remodeling in response to AngII, and this effect may mainly be exhibited in cardiomyocytes.

ZBTB20 overexpression in hearts aggravates adverse cardiac remodeling

We used an AAV9 delivery system to overexpress ZBTB20 in mouse hearts to evaluate the role of this protein in cardiac remodeling. The protein level of ZBTB20 was increased in both the ZBTB20-NS group and the ZBTB20-AngII group, and the level of ZBTB20 was higher in the ZBTB20-AngII group than in the NC-AngII group (Fig. 2a). Four weeks after AngII infusion, the heart and lung weights were higher in the ZBTB20 group than in the NC mouse group, indicative of cardiac hypertrophy and pulmonary edema in the ZBTB20 group. However, the heart and lung weights were not different in the ZBTB20 group injected with NS (Fig. 2b). Following 4 weeks of AngII infusion, H&E staining revealed dilation of the left ventricular (LV) wall and increased cardiomyocyte hypertrophy in the ZBTB20 group compared with the NC group (Fig. 2c). Furthermore, after 4 weeks of AngII treatment, adverse remodeling molecular markers, including atrial natriuretic peptide (Anp), brain natriuretic peptide (Bnp), and myosin heavy chain beta (β-Mhc), showed increased transcription in the ZBTB20 group compared with the NC group (Fig. 2d). Following PSR staining, more severe perivascular and interstitial fibrosis was observed, with a higher LV collagen volume in the ZBTB20 group than in the NC group after AngII infusion (Fig. 2e). Fibrosis molecular markers, including collagen I, collagen III, and smooth muscle actin α (α-SMA), showed increased transcription in the ZBTB20 group. These data indicate that ZBTB20 promotes the progression of adverse cardiac remodeling toward heart failure.

ZBTB20 overexpression in the heart reduced cardiac function

Cardiac dysfunction is a main symptom of heart failure. Cardiac function was evaluated via echocardiography and a pressure–volume loop. Four weeks after AngII infusion, the LV end diastolic diameter (LVEDd) and LV end systolic diameter (LVESd) were increased in the ZBTB20 group, while the LV ejection fraction (EF) and fractional shortening (FS) were reduced compared with those in the NC

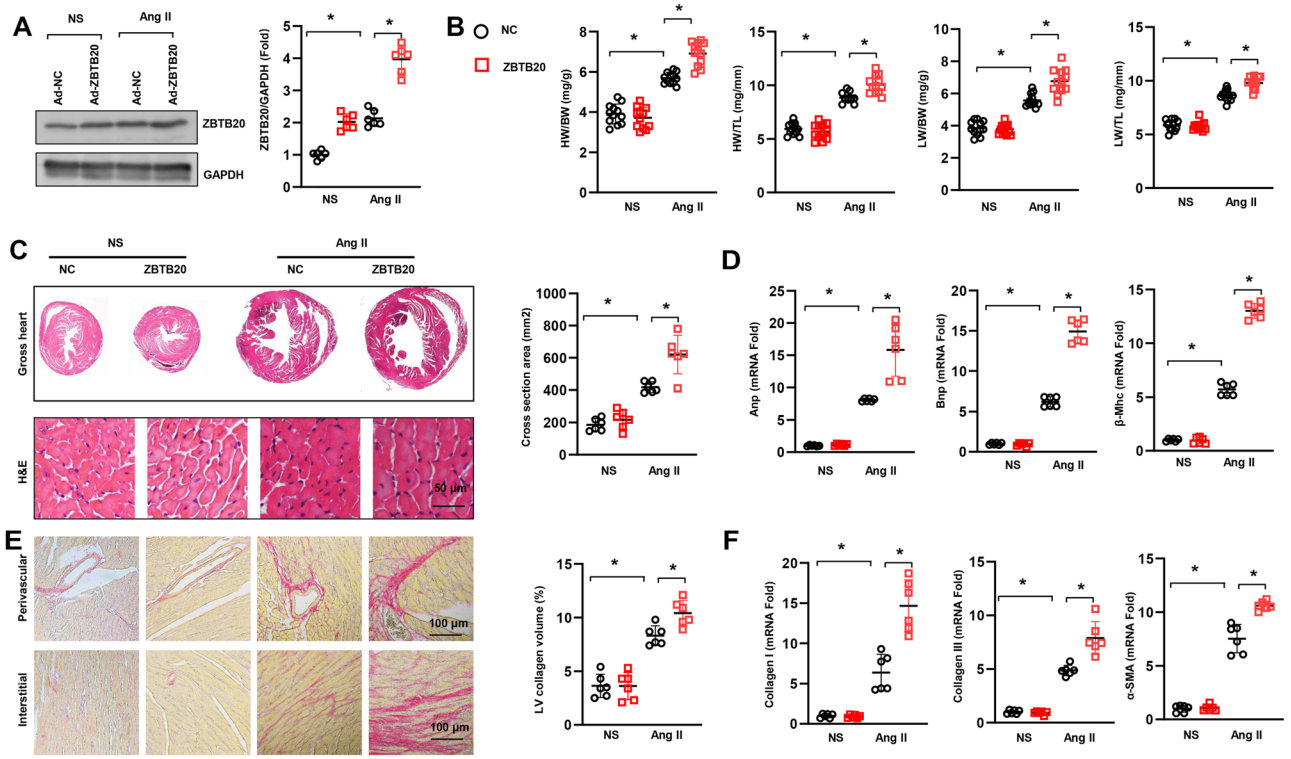

Fig. 2 ZBTB20 overexpression in hearts aggravates adverse cardiac remodeling. **a** ZBTB20 protein levels in mouse hearts after injection of AAV9-ZBTB20 in the indicated group (n = 6). **b** Heart weight (HW)/body weight (BW), heart weight (HW)/tibia length (TL), lung weight (LW)/body weight (BW), and LW/TL (n = 12) in mice subjected to AngII infusion. **c** H&E staining in each group (n = 6). **d** Transcription levels of the fetal genes (n = 6). **e** PSR staining in each group (n = 6). **f** Transcription levels of the fibrosis genes (n = 6). $^{*}P < 0.05$. NC negative control, NS normal saline. Two-way analysis of variance followed by Tukey's post hoc test is shown in Fig. 2a–f

group (Fig. 3a–c). The LV end systolic pressure (ESP) and end diastolic pressure (ESP) were also sharply increased in the ZBTB20 group treated with AngII compared with the NC group treated with AngII (Fig. 3d). In contrast, the LV maximum rate of pressure rise and fall (dp/dt max, dp/dt min) was decreased in the ZBTB20 group compared with the NC group (Fig. 3e). We also detected cardiac inflammation and oxidative stress. As shown in Fig. S1, AngII increased CD68-labeled macrophage infiltration and enhanced the mRNA levels of TNF-α and IL-1 in mouse hearts. While ZBTB20 did not significantly reduce the CD68-labeled macrophage number or the TNF-α and IL-1 mRNA levels (Fig. S1a, b), ZBTB20 reduced the IL-6 level in mouse hearts after AngII infusion (Fig. S1c). We also detected the reactive oxygen species (ROS) level in mouse hearts by 4-HNE staining. AngII increased the lipid peroxidation intermediate metabolite 4-HNE, but ZBTB20 did not reduce the 4-HNE level under AngII insult (Fig. S1d).

ZBTB20 affects the hypertrophic response of cardiomyocytes to AngII

Alterations in ZBTB20 expression following AngII insult were mainly observed in cardiomyocytes. We used NRCM to investigate the role of ZBTB20 in cardiomyocytes. NRCMs were transfected with Ad-ZBTB20 to overexpress ZBTB20 or transfected with ZBTB20 siRNA to silence this protein. The efficiency of these interventions was verified by western blotting (Fig. 4a, b). α-Actin staining results revealed that in cells transfected with ZBTB20, the hypertrophic response was more aggressive than that in cells transfected with the negative control. Furthermore, cells in the ZBTB20 group showed a larger cell surface area and higher transcription of Anp and β-Mhc (Fig. 4c, d). However, in cells transfected with ZBTB20 siRNA, the hypertrophic response was lower than that observed in the cells transfected with scRNA. Moreover, the cells in the ZBTB20 siRNA group showed a smaller surface area and lower transcription of Anp and β-Mhc (Fig. 4e, f).

ZBTB20 activates EGFR and Akt signaling

A previous study showed that ZBTB20 affects EGFR signaling [13]. In this study, we determined whether ZBTB20 plays a role in adverse cardiac remodeling through EGFR. Increased Akt phosphorylation was observed in ZBTB20-overexpressing mouse hearts compared with control mouse hearts after the tissues were treated with AngII (Fig. 5a). Furthermore, the downstream protein mammalian target of rapamycin (mTOR) was more phosphorylated in ZBTB20-overexpressing mouse hearts than in control mouse hearts (Fig. 5a). The phosphorylation level of EGFR, upstream of Akt, was also increased in ZBTB20-overexpressing mouse hearts following AngII infusion compared with control mouse hearts following AngII infusion (Fig. 5b). Since ZBTB20 is a transcription factor, we next evaluated the mRNA level of EGFR. As shown in Fig. 5c, the mRNA level of EGFR was noticeably increased in ZBTB20-overexpressing mouse hearts following AngII infusion (Fig. 5b). Furthermore, a luciferase reporter assay showed that ZBTB20 overexpression dramatically increased the

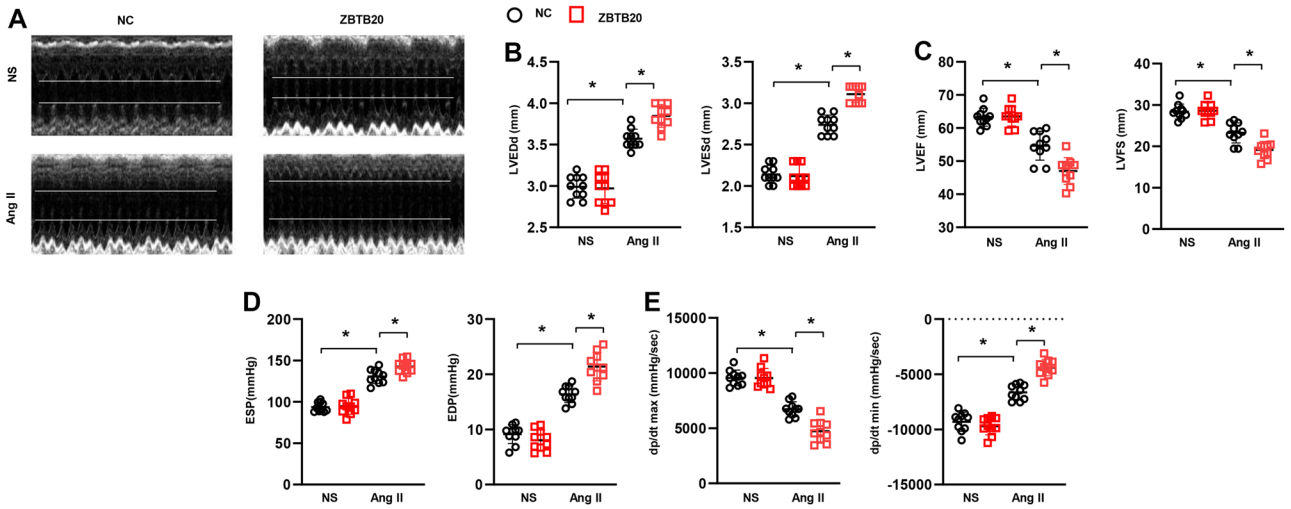

Fig. 3 ZBTB20 overexpression in hearts reduced cardiac function. Representative echocardiography (**a**) and echocardiography data (**b**, **c**) of mice subjected to AngII infusion (n = 10). LVEDd left ventricular end diastolic diameter, LVESd left ventricular end systolic diameter, LVEF left ventricular ejection fraction, LVFS left ventricular fractional shortening. **e** Pressure loop parameters in mice subjected to AngII infusion (n = 10). ESP LV end systolic pressure, EDP end-diastolic pressure, dp/dt max LV maximum rate of pressure rise, dp/dt min LV maximum rate of pressure fall. NC negative control, NS normal saline. $^{*}P < 0.05$. Two-way analysis of variance followed by Tukey's post hoc test is shown in Fig. 3b–e

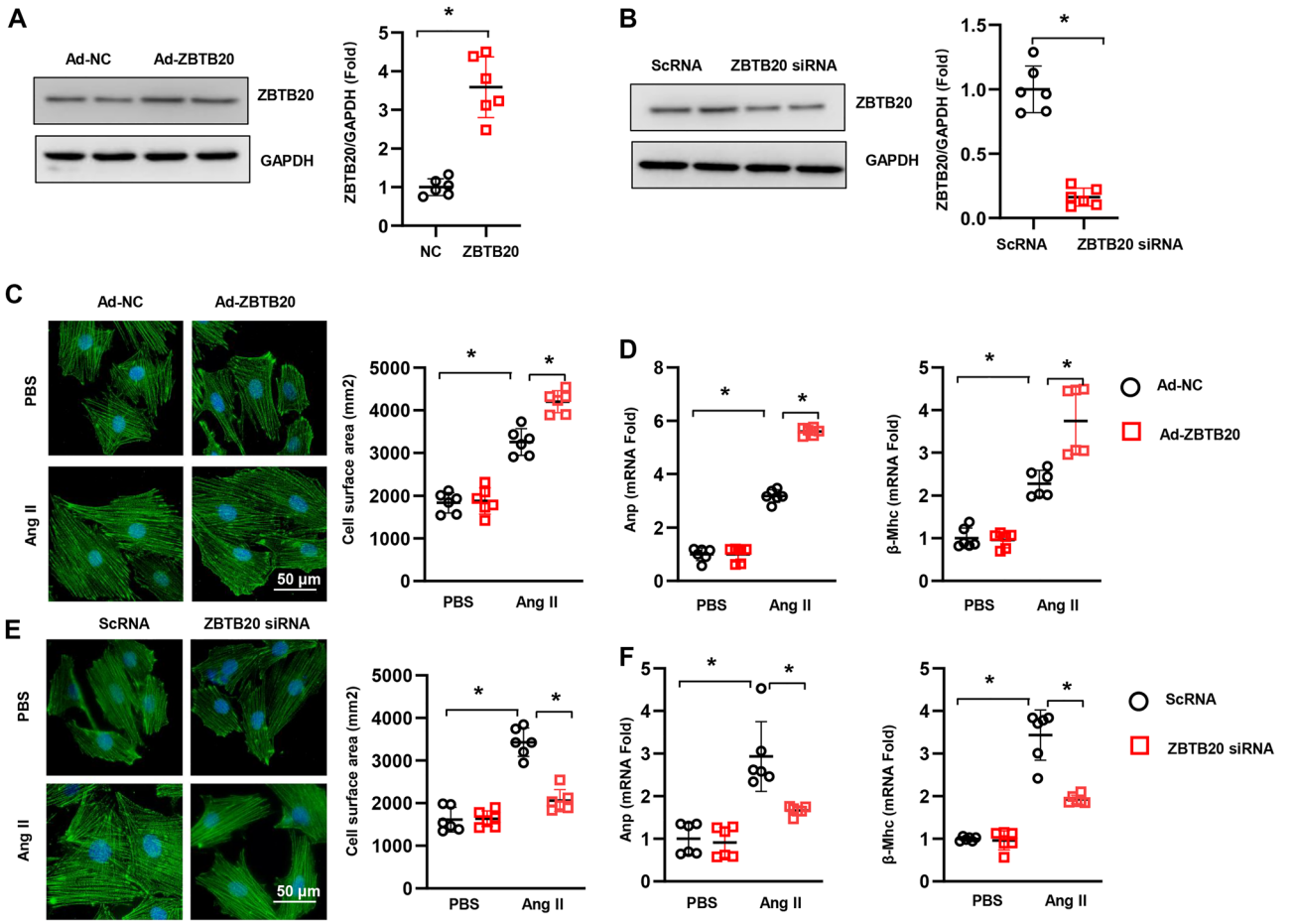

Fig. 4 ZBTB20 affects the hypertrophic response of cardiomyocytes to AngII. **a** ZBTB20 protein levels in cardiomyocytes transfected with Ad-ZBTB20. **b** ZBTB20 protein levels in NRCMs transfected with ZBTB20 siRNA. **c** α-Actin staining of cells transfected with Ad-ZBTB20 and treated with AngII. **d** Transcription levels of these fetal genes in cardiomyocytes transfected with Ad-ZBTB20. **e** α-Actin staining of cells transfected with ZBTB20 siRNA and treated with AngII. **f** Transcription levels of the fetal genes in cardiomyocytes transfected with ZBTB20 siRNA. Each in vitro experiment was performed in triplicate. NC negative control. $*P<0.05$. Unpaired Student's *t*-tests are shown in Fig. 4a, b. Two-way analysis of variance followed by Tukey's post hoc test is shown in Fig. 4c–f

transcriptional activity of the EGFR promoter, while ZBTB20 silencing reduced the transcriptional activity of this promoter under both normal conditions and AngII insult (Fig. 5d, e).

EGFR inhibitor and Akt silencing rescues the deteriorating effects of ZBTB20 in vitro

To investigate the role of the EGFR-Akt pathway in cardiac remodeling, NRCMs were pretreated with erlotinib, an EGFR inhibitor. NRCMs were also infected with Akt siRNA to silence Akt (Fig. 6a). As a result, both EGFR inhibition and Akt siRNA could counteract the aggressive effect of Ad-ZBTB20 in NRCMs following AngII-induced insult (Fig. 6b, c). The cell surface area and mRNA levels of Anp and β-Mhc were reduced in the erlotinib and Ad-ZBTB20 + Akt siRNA groups compared with the Ad-ZBTB20 group (Fig. 6b, c).

Continuous activation of Akt counteracts the protective effects of ZBTB20 knockdown in vivo

We hypothesized that ZBTB20 knockdown would hamper the progression of adverse cardiac remodeling. Mice were injected with AAV9-shZBTB20 to knockdown ZBTB20 in mouse hearts (Fig. 7a, b) and Ad-ca. Akt to achieve constant Akt activity in mouse hearts (Fig. 7a, b). Four weeks after AngII infusion, the heart and lung weights were reduced in the shZBTB20 group compared with the NC group (Fig. 7c). Furthermore, ZBTB20 knockdown hampered the hypertrophic response and fibrosis levels (Fig. 7d, e). Finally, cardiac dysfunction improved in the shZBTB20 group compared with the NC group (Fig. 7f, g). In contrast, continuous Akt activation blocked the protective effects of ZBTB20 knockdown. The hypertrophic response, fibrosis levels, and cardiac function deteriorated when mice were

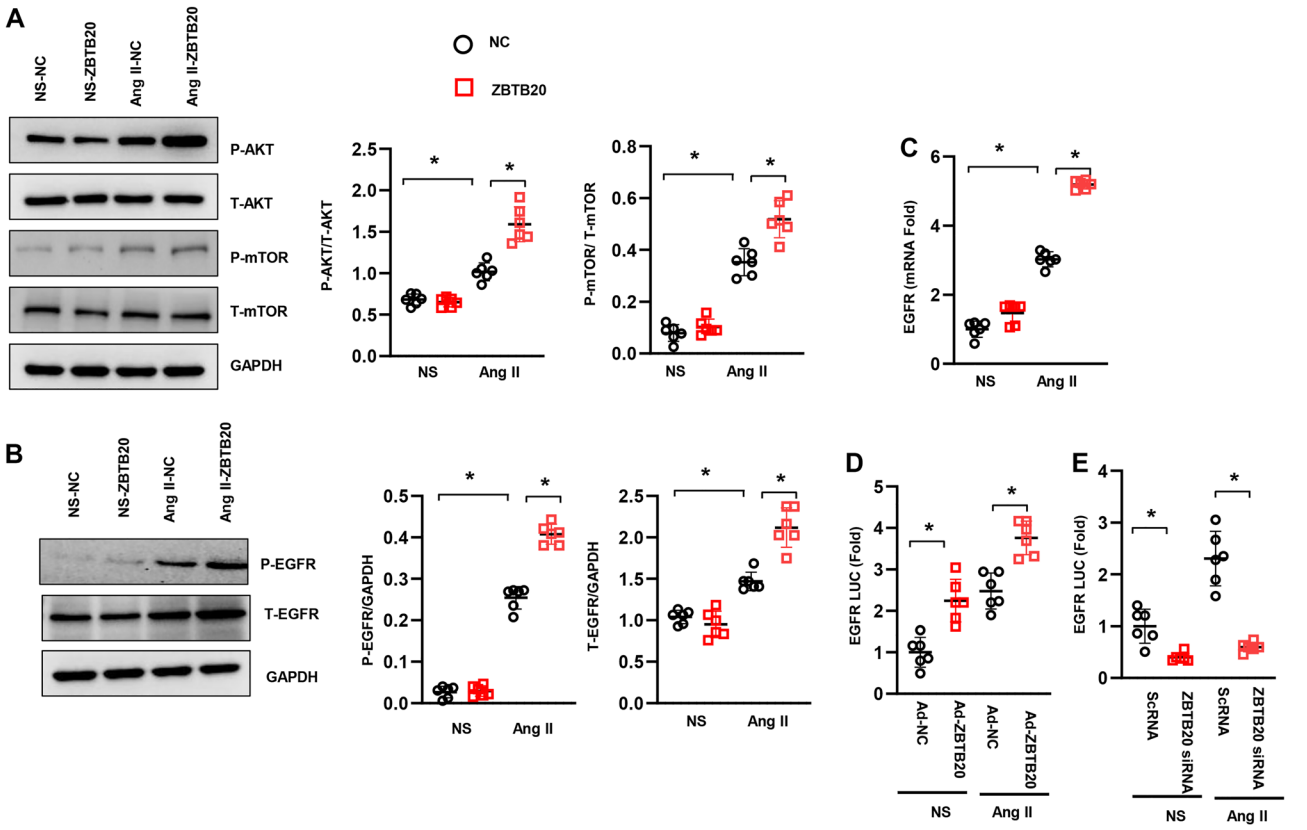

Fig. 5 ZBTB20 activates EGFR and Akt signaling. **a** Protein levels of phosphorylated (P-) and total (T-) Akt as well as mTOR protein levels in mouse hearts following AAV9-ZBTB20 and AngII infusion (n = 6). **b** Protein levels of P- and T-EGFR (n = 6) in mouse hearts. **c** Transcription levels of EGFR in mouse hearts (n = 6). Luciferase activity of EGFR in cardiomyocytes transfected with Ad-ZBTB20 (**d**) or ZBTB20 siRNA (**e**). $^*P < 0.05$. NC negative control, NS normal saline. Two-way analysis of variance followed by Tukey's post hoc test is shown in Fig. 5a–e

subjected to both continuous Akt activation and ZBTB20 knockdown (Fig. 7c–g). Therefore, these findings indicate that the EGFR-Akt pathway is the target of ZBTB20 in the process of cardiac remodeling.

Discussion

ZBTB20 is a member of the BTB/POZ family of transcription factors and functions as a transcriptional repressor while also being involved in numerous diseases, such as brain injury, cancer development, and hepatic lipogenesis [9]. Here, we report that ZBTB20 is highly expressed in heart tissue and is upregulated during the development of adverse cardiac remodeling following heart failure. Second, ZBTB20 exerted deleterious effects during the process of adverse cardiac remodeling, as ZBTB20 overexpression accelerated cardiac hypertrophy, fibrosis, and dysfunction in response to AngII. Third, ZBTB20 regulated the transcription of EGFR and activated the Akt pathway, thus promoting a hypertrophic response. Furthermore, we observed that ZBTB20 knockdown could hamper the process of adverse cardiac remodeling. Thus, ZBTB20 may represent a promising therapeutic target for the inhibition of adverse cardiac remodeling following heart failure.

We have shown that ZBTB20 is expressed in the mouse heart and upregulated following AngII insults. ZBTB20 was expressed in cardiomyocytes, fibroblasts, and endothelial cells in heart tissue. However, after AngII treatment, ZBTB20 was mainly upregulated in cardiomyocytes. Using an in vitro setup, we showed that ZBTB20 overexpression accelerated AngII-induced cardiomyocyte hypertrophy and the expression of fetal genes (Anp and β-Mhc). However, ZBTB20 silencing in cardiomyocytes inhibited these hypertrophic responses to AngII. These results suggest that ZBTB20 may represent a prohypertrophic factor that regulates cardiomyocytes in the heart. Although pathological hypertrophy is initially induced as a compensatory response characterized by concentric growth of the ventricle, this type of hypertrophy progresses to ventricular chamber dilatation with wall thinning through lengthening of individual cardiomyocytes, contractile dysfunction, and heart failure [20, 21]. Previously, other Krüppel-like zinc-finger

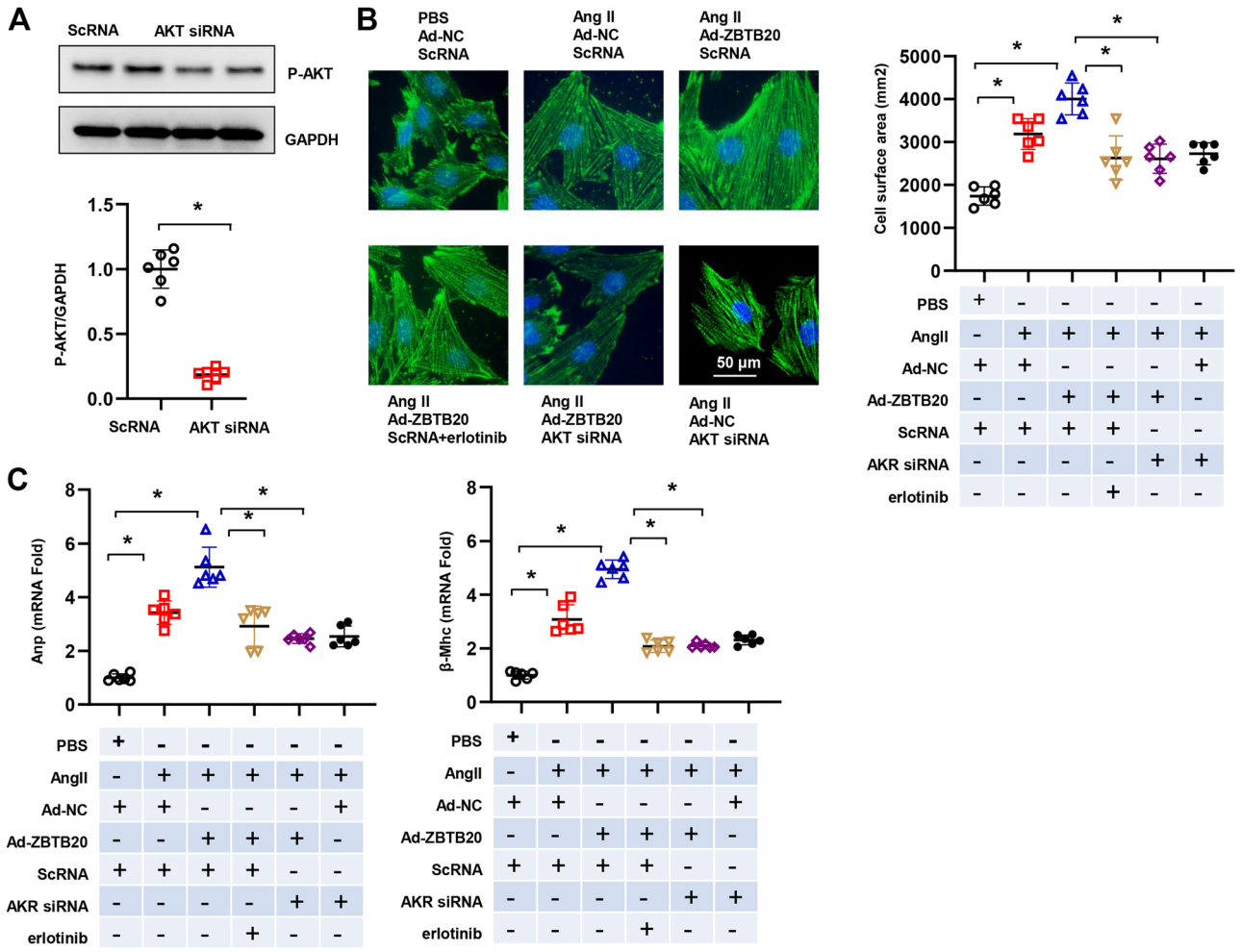

Fig. 6 EGFR inhibitor and Akt silencing rescue the deteriorating effects of ZBTB20 in vitro. **a** Protein levels of P-Akt in NRCMs transfected with Akt siRNA. **b** α-Actin staining of NRCMs transfected with Ad-ZBTB20 or Akt siRNA or pretreated with erlotinib. **c** Transcription levels of the fetal genes in NRCMs. Each in vitro experiment was performed in triplicate. $^*P < 0.05$. Unpaired Student's *t*-tests were used in Fig. 6a. One-way analysis of variance followed by Tukey's post hoc test is shown in Fig. 6b, c

transcription factors have been reported to be associated with AngII-induced cardiac remodeling. BTEB2 was found to be a target of AngII signaling and promoted cardiovascular remodeling [22]. Zinc-finger protein 418 was also found to protect against cardiac hypertrophy and fibrosis [23]. In our previous study, ZBTB20 was shown to protect against adverse cardiac remodeling after myocardial infarction by regulating the oxidative stress-tumor necrosis factor α pathway [24]. Recently, Ren reported that ZBTB20 deficiency led to a marked reduction in heart size, left ventricular wall thickness, and cardiomyocyte size [14]. This information suggests that ZBTB20 is an important regulator of cardiac growth and hypertrophy. In our study, we showed that ZBTB20 overexpression during the progression of adverse cardiac remodeling led to a marked increase in heart size, left ventricular wall thickness, dilation, and cardiac dysfunction. These findings are consistent with those of An-Jing Ren's study, supporting the role of ZBTB20 in cardiac growth. We hypothesize that a high level of ZBTB20 helps the heart undergo pathological growth and leads to hypertrophy. We also detected inflammation and lipid peroxidation in our model and found that ZBTB20 did not significantly influence inflammation and lipid peroxidation during AngII insult, which is quite different from our previous study in a myocardial infarction mouse model [24]. This paradox between the present study and our previous study may be accounted for by the difference between the etiologies of cardiac remodeling. Inflammation and oxidative stress are the initial causes that contribute to cardiac remodeling during myocardial ischemic injury, while in the AngII-induced cardiac remodeling process, hypertrophic signaling is one of the initial causes of cardiac remodeling.

EGFR, also known as ErbB1, is a receptor tyrosine kinase that belongs to the ErbB family [25]. When its ligands, EGF

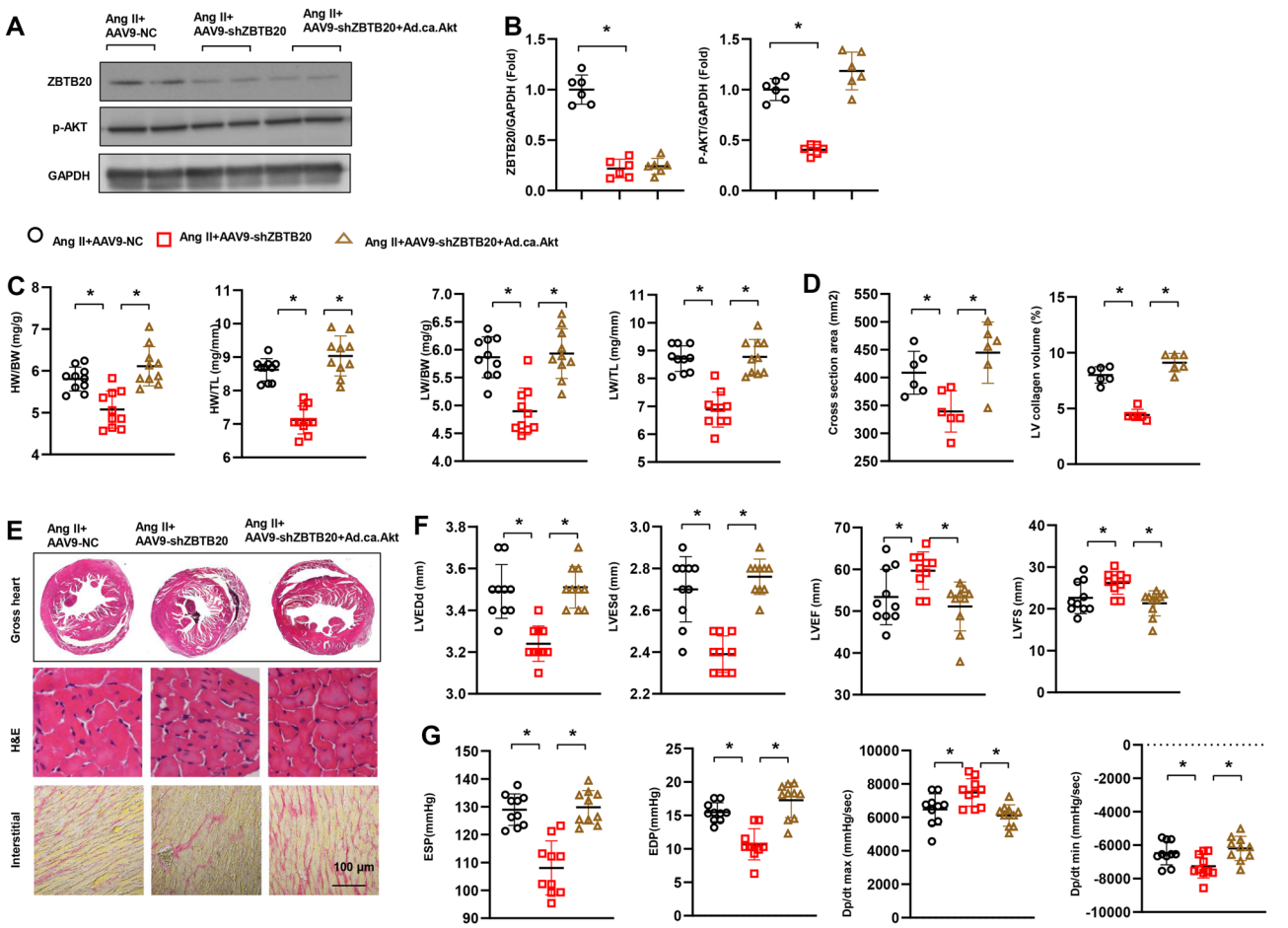

Fig. 7 Continuous activation of Akt counteracts the protective effects of ZBTB20 knockdown in vivo. **a** and **b** ZBTB20 and P-Akt protein levels in mouse hearts following injection with AAV9-shZBTB20 and/or Ad-ca. Akt (n = 6). **c** Heart weight (HW)/body weight (BW), heart weight (HW)/tibia length (TL), lung weight (LW)/body weight (BW), and LW/TL (n = 10) in mice subjected to AngII infusion. **d** Cell cross-sectional area and LV collagen volume in mouse hearts in each group (n = 6). **e** H&E staining in each group (n = 6). **f** Echocardiography data (n = 10). **g** Pressure loop parameters (n = 10). $^*P < 0.05$. NC negative control, Ad-ca. Akt adenovirus vectors carrying constitutively active AKT1. Unpaired Student's *t*-tests were used in Fig. 7b. One-way analysis of variance followed by Tukey's post hoc test is shown in Fig. 7c–g

and heparin, bind to a receptor, phosphorylation occurs, which allows EGFR to recruit adapter signaling molecules such as Akt and ERK [26]. In 2016, Peng et al. [27] discovered the role of EGFR in AngII-induced cardiac hypertrophy. Smith et al. [28] also highlighted the importance of EGFR transactivation in AngII-AT1R-mediated cardiomyocyte hypertrophy. Thus, blocking EGFR is a promising method to treat cardiac hypertrophy [5, 29]. In our study, both total-Akt and EGFR were upregulated in ZBTB20-overexpressing mouse hearts when exposed to AngII. Furthermore, we observed that ZBTB20 increased EGFR transcriptional activity and consequently led to increased EGFR phosphorylation. These results demonstrated further activation of the downstream target Akt, indicating that ZBTB20 regulates adverse cardiac remodeling via the EGFR pathway. Sustained activation of Akt was observed in ZBTB20-overexpressing mouse hearts under AngII insult. Continuous activation of Akt was shown to lead to pathological cardiac hypertrophy [30]. Thus, the ZBTB20-EGFR-Akt pathway explains the pro-adverse remodeling effect of ZBTB20. The hypothesis that knockdown of ZBTB20 would inhibit the cardiac remodeling process in response to AngII was confirmed in our rescue experiment. However, when we continuously activated Akt, this protective effect of ZBTB20 knockdown was abolished.

This study illustrated the essential role of ZBTB20 in adverse cardiac remodeling and that this effect of ZBTB20 was mediated by regulating the EGFR-Akt pathway. When ZBTB20 was knocked down, adverse remodeling in response to AngII was hampered. Thus, ZBTB20 may represent a promising therapeutic target for new heart failure treatment strategies.

Supplementary information The online version contains supplementary material available at https://doi.org/10.1007/s00109-021-02103-0.

Author contribution LF and LQ contributed to the study conception and designed the experiments; LF, YM, WZ, and ZH carried out the experiments; WX and DM analyzed the experimental results; and LF, LQ and WZ wrote and revised the manuscript.

Funding This research was supported by the National Natural Science Foundation of China (Grant No. 81900216) and the Science and Technology Program of Xuzhou KC18173.

Availability of data and material All data will be available upon request from the corresponding author.

Declarations

Ethics approval The Guide for the Care and Use of Laboratory Animals published by the US National Institutes of Health was applied to all animal procedures in our experiment, and approval from the Institutional Animal Care and Use Committee at Xuzhou Medical University (Xuzhou, China; Approval number: JSXZ-2018–1012-007; Approval data: 12/10/2018) was also acquired.

Conflict of interest The authors declare no conflicts of interest.

References

1. Schuttler D, Clauss S, Weckbach LT, Brunner S (2019) Molecular mechanisms of cardiac remodeling and regeneration in physical exercise. Cells 8:1128. https://doi.org/10.3390/cells8101128
2. Ames MK, Atkins CE, Pitt B (2019) The renin-angiotensin-aldosterone system and its suppression. J Vet Intern Med 33:363–382. https://doi.org/10.1111/jvim.15454
3. Rossignol P, Hernandez AF, Solomon SD, Zannad F (2019) Heart failure drug treatment. Lancet 393:1034–1044. https://doi.org/10.1016/S0140-6736(18)31808-7
4. Grisanti LA, Guo S, Tilley DG (2017) Cardiac GPCR-mediated EGFR transactivation: impact and therapeutic implications. J Cardiovasc Pharmacol 70:3–9. https://doi.org/10.1097/FJC.0000000000000462
5. Liang D, Zhong P, Hu J, Lin F, Qian Y, Xu Z, Wang J, Zeng C, Li X, Liang G (2015) EGFR inhibition protects cardiac damage and remodeling through attenuating oxidative stress in STZ-induced diabetic mouse model. J Mol Cell Cardiol 82:63–74. https://doi.org/10.1016/j.yjmcc.2015.02.029
6. Liu L, Jin X, Hu CF, Zhang YP, Zhou Z, Li R, Shen CX (2018) Amphiregulin enhances cardiac fibrosis and aggravates cardiac dysfunction in mice with experimental myocardial infarction partly through activating EGFR-dependent pathway. Basic Res Cardiol 113:12. https://doi.org/10.1007/s00395-018-0669-y
7. Liu X, Lin L, Li Q, Ni Y, Zhang C, Qin S, Wei J (2019) ERK1/2 communicates GPCR and EGFR signaling pathways to promote CTGF-mediated hypertrophic cardiomyopathy upon Ang-II stimulation. BMC Mol Cell Biol 20:14. https://doi.org/10.1186/s12860-019-0202-7
8. Zuo C, Li X, Huang J, Chen D, Ji K, Yang Y, Xu T, Zhu D, Yan C, Gao P (2018) Osteoglycin attenuates cardiac fibrosis by suppressing cardiac myofibroblast proliferation and migration through antagonizing lysophosphatidic acid 3/matrix metalloproteinase 2/epidermal growth factor receptor signalling. Cardiovasc Res 114:703–712. https://doi.org/10.1093/cvr/cvy035
9. Doeppner TR, Herz J, Bahr M, Tonchev AB, Stoykova A (2019) Zbtb20 regulates developmental neurogenesis in the olfactory bulb and gliogenesis after adult brain injury. Mol Neurobiol 56:567–582. https://doi.org/10.1007/s12035-018-1104-y
10. Liu G, Zhou L, Zhang H, Chen R, Zhang Y, Li L, Lu JY, Jiang H, Liu D, Qi S et al (2017) Regulation of hepatic lipogenesis by the zinc finger protein Zbtb20. Nat Commun 8:14824. https://doi.org/10.1038/ncomms14824
11. Sun Y, Preiss NK, Valenteros KB, Kamal Y, Usherwood YK, Frost HR, Usherwood EJ (2020) Zbtb20 restrains CD8 T cell immunometabolism and restricts memory differentiation and antitumor immunity. J Immunol 205:2649–2666. https://doi.org/10.4049/jimmunol.2000459
12. Zhang Y, Zhou X, Zhang M, Cheng L, Zhang Y, Wang X (2019) ZBTB20 promotes cell migration and invasion of gastric cancer by inhibiting IkappaBalpha to induce NF-kappaB activation. Artif Cells Nanomed Biotechnol 47:3862–3872. https://doi.org/10.1080/21691401.2019.1670188
13. Zhang H, Shi JH, Jiang H, Wang K, Lu JY, Jiang X, Ma X, Chen YX, Ren AJ, Zheng J et al (2018) ZBTB20 regulates EGFR expression and hepatocyte proliferation in mouse liver regeneration. Cell Death Dis 9:462. https://doi.org/10.1038/s41419-018-0514-0
14. Ren AJ, Chen C, Zhang S, Liu M, Wei C, Wang K, Ma X, Song Y, Wang R, Zhang H et al (2020) Zbtb20 deficiency causes cardiac contractile dysfunction in mice. FASEB J 34:13862–13876. https://doi.org/10.1096/fj.202000160RR
15. Karbach SH, Schonfelder T, Brandao I, Wilms E, Hormann N, Jackel S, Schuler R, Finger S, Knorr M, Lagrange J et al (2016) Gut microbiota promote angiotensin II-induced arterial hypertension and vascular dysfunction. J Am Heart Assoc 5:e003698. https://doi.org/10.1161/JAHA.116.003698
16. Kvakan H, Kleinewietfeld M, Qadri F, Park JK, Fischer R, Schwarz I, Rahn HP, Plehm R, Wellner M, Elitok S et al (2009) Regulatory T cells ameliorate angiotensin II-induced cardiac damage. Circulation 119:2904–2912. https://doi.org/10.1161/CIRCULATIONAHA.108.832782
17. Muller DN, Dechend R, Mervaala EM, Park JK, Schmidt F, Fiebeler A, Theuer J, Breu V, Ganten D, Haller H et al (2000) NF-kappaB inhibition ameliorates angiotensin II-induced inflammatory damage in rats. Hypertension 35:193–201. https://doi.org/10.1161/01.hyp.35.1.193
18. Zong J, Li FF, Liang K, Dai R, Zhang H, Yan L, Liu JL, Xu LH, Qian WH (2018) Nuclear localization leucine-rich-repeat protein 1 deficiency protects against cardiac hypertrophy by pressure overload. Cell Physiol Biochem 48:75–86. https://doi.org/10.1159/000491664
19. Li F, Zhang H, Yang L, Yong H, Qin Q, Tan M, Xu L, Liang K, Zong J, Qian W (2018) NLRP3 deficiency accelerates pressure overload-induced cardiac remodeling via increased TLR4 expression. J Mol Med (Berl) 96:1189–1202. https://doi.org/10.1007/s00109-018-1691-0
20. Nakamura M, Sadoshima J (2018) Mechanisms of physiological and pathological cardiac hypertrophy. Nat Rev Cardiol 15:387–407. https://doi.org/10.1038/s41569-018-0007-y
21. Shimizu I, Minamino T (2016) Physiological and pathological cardiac hypertrophy. J Mol Cell Cardiol 97:245–262. https://doi.org/10.1016/j.yjmcc.2016.06.001
22. Shindo T, Manabe I, Fukushima Y, Tobe K, Aizawa K, Miyamoto S, Kawai-Kowase K, Moriyama N, Imai Y, Kawakami H et al (2002) Kruppel-like zinc-finger transcription factor KLF5/BTEB2 is a target for angiotensin II signaling and an essential regulator of cardiovascular remodeling. Nat Med 8:856–863. https://doi.org/10.1038/nm738

23. Pan L, Sheng M, Huang Z, Zhu Z, Xu C, Teng L, He L, Gu C, Yi C, Li J (2017) Zinc-finger protein 418 overexpression protects against cardiac hypertrophy and fibrosis. PLoS One 12:e0186635. https://doi.org/10.1371/journal.pone.0186635
24. de Vicente LG, Pinto AP, da Rocha AL, Pauli JR, de Moura LP, Cintra DE, Ropelle ER, da Silva ASR (2020) Role of TLR4 in physical exercise and cardiovascular diseases. Cytokine 136:155273. https://doi.org/10.1016/j.cyto.2020.155273
25. Shah S, Akhtar MS, Hassan MQ, Akhtar M, Paudel YN, Najmi AK (2018) EGFR tyrosine kinase inhibition decreases cardiac remodeling and SERCA2a/NCX1 depletion in streptozotocin induced cardiomyopathy in C57/BL6 mice. Life Sci 210:29–39. https://doi.org/10.1016/j.lfs.2018.08.018
26. Childers CL, Tessier SN, Storey KB (2019) The heart of a hibernator: EGFR and MAPK signaling in cardiac muscle during the hibernation of thirteen-lined ground squirrels. Ictidomys tridecemlineatus PeerJ 7:e7587. https://doi.org/10.7717/peerj.7587
27. Peng K, Tian X, Qian Y, Skibba M, Zou C, Liu Z, Wang J, Xu Z, Li X, Liang G (2016) Novel EGFR inhibitors attenuate cardiac hypertrophy induced by angiotensin II. J Cell Mol Med 20:482–494. https://doi.org/10.1111/jcmm.12763
28. Smith NJ, Chan HW, Qian H, Bourne AM, Hannan KM, Warner FJ, Ritchie RH, Pearson RB, Hannan RD, Thomas WG (2011) Determination of the exact molecular requirements for type 1 angiotensin receptor epidermal growth factor receptor transactivation and cardiomyocyte hypertrophy. Hypertension 57:973–980. https://doi.org/10.1161/HYPERTENSIONAHA.110.166710
29. De Pasquale V, Pezone A, Sarogni P, Tramontano A, Schiattarella GG, Avvedimento VE, Paladino S, Pavone LM (2018) EGFR activation triggers cellular hypertrophy and lysosomal disease in NAGLU-depleted cardiomyoblasts, mimicking the hallmarks of mucopolysaccharidosis IIIB. Cell Death Dis 9:40. https://doi.org/10.1038/s41419-017-0187-0
30. Bodine SC, Stitt TN, Gonzalez M, Kline WO, Stover GL, Bauerlein R, Zlotchenko E, Scrimgeour A, Lawrence JC, Glass DJ et al (2001) Akt/mTOR pathway is a crucial regulator of skeletal muscle hypertrophy and can prevent muscle atrophy in vivo. Nat Cell Biol 3:1014–1019. https://doi.org/10.1038/ncb1101-1014